Lawrence Berkeley National Laboratory

Title

Transverse momentum dependent shape function for J/ψ production in SIDIS

Authors

Boer, Daniël
Bor, Jelle
Maxia, Luca
et al.

Peer reviewed

Transverse momentum dependent shape function for J/ψ production in SIDIS

Daniël Boer,[a] **Jelle Bor,**[a,b] **Luca Maxia,**[a] **Cristian Pisano**[c,d] **and Feng Yuan**[e]

[a] *Van Swinderen Institute for Particle Physics and Gravity, University of Groningen,*
Nijenborgh 4, 9747 AG Groningen, The Netherlands

[b] *IJCLab, CNRS, Université Paris-Saclay,*
91405 Orsay, France

[c] *Dipartimento di Fisica, Università di Cagliari,*
Cittadella Universitaria, I-09042 Monserrato (CA), Italy

[d] *INFN, Sezione di Cagliari,*
Cittadella Universitaria, I-09042 Monserrato (CA), Italy

[e] *Nuclear Science Division, Lawrence Berkeley National Laboratory,*
Berkeley, CA 94720, U.S.A.

E-mail: d.boer@rug.nl, j.bor@rug.nl, l.maxia@rug.nl,
cristian.pisano@unica.it, fyuan@lbl.gov

ABSTRACT: It has been shown previously that the transverse momentum dependent (TMD) factorization of heavy quarkonium production requires a TMD shape function. Its perturbative tail can be extracted by matching the cross sections valid at low and high transverse momenta. In this article we compare the order-α_s TMD expressions with the order-α_s^2 collinear ones for J/ψ production in semi-inclusive deep inelastic scattering (SIDIS), employing nonrelativistic QCD in both cases. In contrast to previous studies, we find that the small transverse momentum limit of the collinear expressions contains discontinuities. We demonstrate how to properly deal with them and include their finite contributions to the TMD shape functions. Moreover, we show that soft gluon emission from the low transverse momentum Born diagrams provide the same leading order TMD shape functions as required for the matching. Their revised perturbative tails have a less divergent behavior as compared to the TMD fragmentation functions of light hadrons. Finally, we investigate the universality of TMD shape functions in heavy quarkonium production, identify the need for process dependent factorization and discuss the phenomenological implications.

KEYWORDS: Quarkonium, Specific QCD Phenomenology, Deep Inelastic Scattering or Small-x Physics

ARXIV EPRINT: 2304.09473

Contents

1 Introduction

In recent years, heavy quarkonium production in various inclusive processes has attracted great interest as a way to probe the transverse momentum dependent (TMD) gluon distributions [1–11]. In this paper, we focus on J/ψ production in semi-inclusive deep inelastic scattering (SIDIS),

$$e(\ell) + p(P) \to e'(\ell') + \gamma^*(q) + p(P) \to e'(\ell') + J/\psi(P_\psi) + X, \tag{1.1}$$

where the particle momenta are given between brackets and the virtual photon momentum is given by $q = \ell - \ell'$. The J/ψ mass $M_\psi^2 = P_\psi^2$ and the photon virtuality $Q^2 = -q^2 > 0$ are considered hard scales in the process, i.e. they are considered much larger than the nonperturbative QCD scale Λ_{QCD}, although most results will also be valid for photoproduction ($Q^2 = 0$). The electron and proton masses will be neglected w.r.t. M_ψ and Q whenever possible. The virtual photon transverse momentum is denoted by $\boldsymbol{q}_T$ and can be directly related to the J/ψ transverse momentum $\boldsymbol{P}_{\psi\perp}$. The distinct subscripts used for the transverse momentum components, specifically "T" and "$\perp$", serve to emphasize the different frames in which they are measured. In particular, we consider $\boldsymbol{q}_T$ when both the target proton and the J/ψ have no transverse components and $\boldsymbol{P}_{\psi\perp}$ when the photon and the proton have only longitudinal components.

Depending on the value of $|\boldsymbol{q}_T|$, we can identify two different transverse momentum regions, see figure 1. The high transverse momentum (HTM) region is given by the condition $|\boldsymbol{q}_T| \gg \Lambda_{\mathrm{QCD}}$, while the low transverse momentum (LTM) region corresponds to $|\boldsymbol{q}_T| \ll \mu_H$. Here $\mu_H = f(Q, M_\psi)$ with $f(Q, M_\psi) \gtrsim M_\psi$ generically denotes the hard scale of the process. The cross section can be evaluated within the two transverse momentum

regions by adopting the proper factorization that enables to separate the short-distance from the long-distance contributions. The collinear factorization is applicable at HTM, while the TMD factorization is expected to be valid at LTM [12], for which the cross section is sensitive to TMD quantities. In addition, we can identify an intermediate transverse momentum (ITM) region, namely $\Lambda_{\mathrm{QCD}} \ll |\boldsymbol{q}_T| \ll \mu_H$, where both factorizations are valid. Since our attention will be mostly directed towards this overlapping region, where $|\boldsymbol{q}_T|$ (or equivalently $|\boldsymbol{P}_{\psi\perp}|$) becomes small compared to the hard scale, we will neglect any transverse momentum dependence in $f(Q, M_\psi)$.

To describe J/ψ hadronization we employ nonrelativistic QCD (NRQCD) [13], in which the heavy-quark pair forms a Fock state, specified by $n = {}^{2S+1}L_J^{[c]}$: S denotes the spin, L the orbital angular momentum, J the total angular momentum and c the color state of the pair. Note that the pair can couple either as a color-singlet (CS), with $c = 1$, or as a color-octet (CO) state, with $c = 8$. The (low-energy) transition from this general state to the J/ψ is encoded in the nonperturbative Long-Distance Matrix Elements (LDMEs) that are distinct for each quarkonium Fock state. States with different quantum numbers n do not interfere as the cross section is proportional to a direct sum of LDMEs, up to a required precision in the expansion w.r.t. v, which corresponds to the (non-relativistic) relative velocity of the heavy quark-antiquark pair in the quarkonium rest frame. In the following we will truncate the expansion up to the relative order v^4, including the ${}^3S_1^{[1]}$ CS state and the ${}^1S_0^{[8]}$, ${}^3S_1^{[8]}$, ${}^3P_J^{[8]}$ CO states. Note that, in the following we will not consider the interference among P-wave states since it is not necessary in the evaluation of the unpolarized differential cross section. However, we have taken them into account in our brief digression on the production of polarized J/ψ mesons in SIDIS (see section 4).

In refs. [14, 15] it was found that the TMD factorized expressions have to take into account final state smearing effects that are encoded in the TMD shape function (TMDShF). This nonperturbative hadronic quantity describes the transition from the heavy quark pair to a bound quarkonium state, which not only contains the formation of the bound state in terms of an LDME, but also the transverse momentum effects that arise from the soft-gluon radiation.

In refs. [16, 17] the matching procedure in SIDIS has been investigated, according to which the TMD and collinear expressions are compared in the ITM region. It was found that the introduction of TMDShFs solves the mismatch between the collinear and TMD expressions, by resumming $|\boldsymbol{q}_T|$ divergences in the Sudakov factor. However, this term is in contradiction with other studies, as it has been demonstrated that no double logarithms in the nonperturbative Sudakov factor associated to heavy quark production are present for $pp \to (J/\psi \text{ or } \Upsilon) + X$ [18] and for open heavy-quark pair production, both in ep [19] and pp [20] collisions. The absence of the double logarithms in J/ψ production can also be seen in ref. [21]. Due to this discrepancy, universality was assumed in [22] using the explicit result of [18]; however, as we will see, this only holds for photoproduction, not electroproduction.

We found that the discrepancy in the ep matching study arises from the presence of discontinuities in the structure functions that appear in the small-$\boldsymbol{q}_T$ limit of collinear factorized expressions. These structure functions contain a Dirac delta function for which a
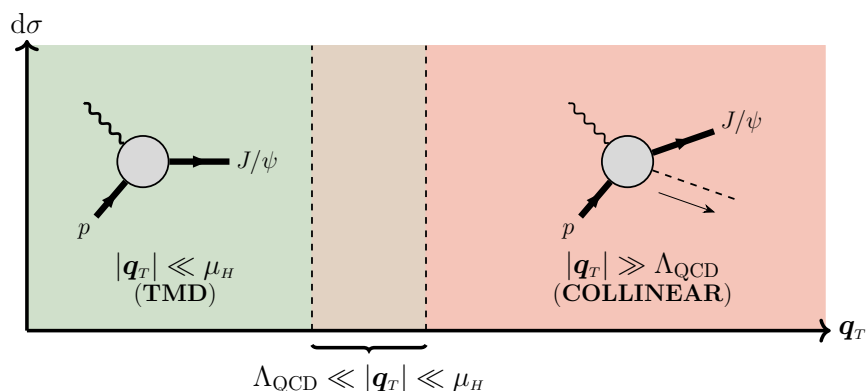
Figure 1. Schematical overview of matching in $ep \to e'J/\psi + X$ to obtain the leading order shape function.

small-$\boldsymbol{q}_T$ approximation is applied. The approximation employed in refs. [16, 17], which is an extension of a well-known expression [23] to the heavy quarkonium case, would be valid when multiplied by a continuous function, but that turns out to be invalid in the present case of discontinuous hard scattering factors. In this article we show how to properly treat these expressions to resolve this discrepancy.

In addition, we extend our analysis to single quarkonium production in pp collisions, where the hard scale is a function of the quarkonium mass only: $\mu_H = f(M_\psi)$ with $f(M_\psi) \sim M_\psi$. This allows us to test the connection of TMDShFs obtained in different cases, i.e. to study their universal properties. Even if we expect that the LDMEs are process independent in the collinear description, the same is not necessarily true for the TMDShFs. Indeed in the latter process dependences may arise due to the transverse momentum exchange with other colored objects.

The paper is organized as follows. In section 2 we revise the matching procedure. In particular, in section 2.1 we discuss the pole structure of the collinear cross section in the small transverse momentum limit in detail, while the new TMDShF results for SIDIS are presented in section 2.2. In section 3 we address the aforementioned process dependence, comparing the TMDShFs in SIDIS and in pp collisions. Conclusions are given in section 4, together with a summary of our findings. In addition, there are two appendices at the end of this paper. In appendix A we present a more complete derivation of our method to include the pole structure contributions in our results. In appendix B we derive the soft gluon emission from the Born amplitude obtained through the eikonal approximation.

2 The matching procedure

The SIDIS reaction in eq. (1.1) is described by the conventional kinematical SIDIS variables

$$x_B = \frac{Q^2}{2P \cdot q}, \quad y = \frac{P \cdot q}{P \cdot \ell}, \quad z = \frac{P \cdot P_\psi}{P \cdot q} . \tag{2.1}$$

We consider a frame where the virtual photon has no transverse momentum component, and we identify two light-cone directions n_+ and n_-, for which $n_+ \cdot n_- = 1$. With these, the Sudakov decomposition of the relevant momenta can be written as

$$P^\mu = n_+^\mu,$$
$$q^\mu = -x_B n_+^\mu + \frac{Q^2}{2x_B} n_-^\mu,$$
$$P_\psi^\mu = \frac{x_B M_{\psi\perp}^2}{zQ^2} n_+^\mu + \frac{zQ^2}{2x_B} n_-^\mu + P_{\psi\perp}^\mu, \tag{2.2}$$

where $P_{\psi\perp}^2 = -\boldsymbol{P}_{\psi\perp}^2$ is the squared J/ψ transverse momentum (w.r.t. the photon and proton), while $M_{\psi\perp} = \sqrt{M_\psi^2 + \boldsymbol{P}_{\psi\perp}^2}$ is the J/ψ transverse mass.

In particular, we will consider the fully unpolarized differential cross section $\mathrm{d}\sigma/(\mathrm{d}x_B \mathrm{d}y \mathrm{d}z \mathrm{d}\boldsymbol{q}_T^2 \mathrm{d}\phi_\psi)$, where ϕ_ψ is the J/ψ azimuthal angle measured w.r.t. the lepton plane. Moreover, we replaced the transverse momentum of the J/ψ with that of the photon $\boldsymbol{q}_T$ (evaluated w.r.t. the hadrons); this replacement is achieved via

$$|\boldsymbol{q}_T| = \frac{1}{z}|\boldsymbol{P}_{\psi\perp}| . \tag{2.3}$$

The differential cross section can be parameterised in the HTM region as follows [16]

$$\frac{\mathrm{d}\sigma}{\mathrm{d}x_B \mathrm{d}y \mathrm{d}z \mathrm{d}\boldsymbol{q}_T^2 \mathrm{d}\phi_\psi} = \frac{\alpha}{yQ^2} \bigg\{ \Big[1 + (1-y)^2\Big] F_{UU,\perp} + 4(1-y)F_{UU,\parallel}$$
$$+ 2(2-y)\sqrt{1-y}\cos\phi_\psi F_{UU}^{\cos\phi_\psi} + 4(1-y)\cos 2\phi_\psi F_{UU}^{\cos 2\phi_\psi} \bigg\}, \tag{2.4}$$

where the first two subscripts of the structure functions F refer to the polarization of the initial (unpolarized) proton and electron. The last subscript in $F_{UU,\mathcal{P}}$ with $\mathcal{P} = \perp, \parallel$ refers to the virtual photon polarization (transverse or longitudinal), while for F_{UU}^Φ with $\Phi = \cos\phi_\psi, \cos 2\phi_\psi$ the superscript refers to the angular term that accompanies it. Henceforth, we will refer to the aforementioned hard scattering structure functions via the general notation $F_{UU,\mathcal{P}}^\Phi$. On the other hand, the same differential cross section evaluated in the LTM region is given by

$$\frac{\mathrm{d}\sigma}{\mathrm{d}x_B \mathrm{d}y \mathrm{d}z \mathrm{d}\boldsymbol{q}_T^2 \mathrm{d}\phi_\psi} = \frac{\alpha}{yQ^2} \bigg\{ \Big[1 + (1-y)^2\Big] \mathcal{F}_{UU,\perp} + 4(1-y)\mathcal{F}_{UU,\parallel} + 4(1-y)\cos 2\phi_\psi \mathcal{F}_{UU}^{\cos 2\phi_\psi} \bigg\}, \tag{2.5}$$

where the structure function $\mathcal{F}_{UU}^{\cos\phi_\psi}$, being subleading power/twist, has not been included. Note the difference in the structure functions: $F_{UU,\mathcal{P}}^\Phi$ are evaluated in collinear factorization, while the calligraphic $\mathcal{F}_{UU,\mathcal{P}}^\Phi$ are calculated within transverse momentum factorization.

2.1 From high to intermediate transverse momentum

In this section we provide a systematic method to investigate the small-$\boldsymbol{q}_T$ limit of SIDIS observables at HTM ($|\boldsymbol{q}_T| \gg \Lambda_{\mathrm{QCD}}$). Adopting the parton model, the production of a J/ψ possessing a high transverse momentum component is possible at the lowest order in α_s via

$$\gamma^*(q) + a(p_a) \to c\bar{c}[n](P_\psi) + a'(p_a'), \tag{2.6}$$

where a can be either a quark, antiquark, or gluon. In this kinematical regime we adopt collinear factorization, for which

$$p_a \approx \xi P \ . \tag{2.7}$$

The perturbative amplitude squared $|\mathcal{M}|^2$ for the hadronic process in eq. (1.1) is obtained by contracting the leptonic tensor $L^{\mu\nu}$ with the amplitude $H_\mu^{(a)[n]}$, describing the partonic process in eq. (2.6), and its conjugate $H_\nu^{(a)[n]*}$. In particular, the lepton tensor can be written as follows:

$$L^{\mu\nu} = \frac{Q^2}{y^2}\left\{\left[1+(1-y)^2\right]\epsilon_\perp^{\mu\nu} + 4(1-y)\left(\epsilon_\parallel^{\mu\nu} + \epsilon_{\cos 2\phi_\psi}^{\mu\nu}\right) + 2(2-y)\sqrt{1-y}\,\epsilon_{\cos\phi_\psi}^{\mu\nu}\right\}, \tag{2.8}$$

where we introduced the tensors

$$\epsilon_\perp^{\mu\nu} = -g_\perp^{\mu\nu}, \quad \epsilon_\parallel^{\mu\nu} = \epsilon_L^\mu \epsilon_L^\nu, \quad \epsilon_{\cos\phi_\psi}^{\mu\nu} = \left(\epsilon_L^\mu \hat{\ell}_\perp^\nu + \hat{\ell}_\perp^\mu \epsilon_L^\nu\right), \quad \epsilon_{\cos 2\phi_\psi}^{\mu\nu} = \left(\hat{\ell}_\perp^\mu \hat{\ell}_\perp^\nu + \frac{1}{2}g_\perp^{\mu\nu}\right). \tag{2.9}$$

Moreover, $g_\perp^{\mu\nu}$ is the transverse projector

$$g_\perp^{\mu\nu} \equiv g^{\mu\nu} - \frac{1}{P\cdot q}\left(P^\mu q^\nu + q^\mu P^\nu\right) - \frac{Q^2}{(P\cdot q)^2}P^\mu P^\nu, \tag{2.10}$$

while $\epsilon_L^\mu(q)$ is the longitudinal polarization vector

$$\epsilon_L^\mu(q) = \frac{1}{Q}\left(q^\mu + \frac{Q^2}{P\cdot q}P^\mu\right), \tag{2.11}$$

and $\hat{\ell}_\perp^\mu$ is the unit vector along the transverse component of ℓ, w.r.t. the photon-proton axis. Henceforth, we refer to one of the tensors in eq. (2.9) via the general notation $\epsilon_{\mathcal{P};\Phi}^{\mu\nu}$, where $\mathcal{P} =\perp, \parallel$ and $\Phi = \cos\phi_\psi, \cos 2\phi_\psi$. Employing this, the structure functions introduced in eq. (2.4) can be evaluated via

$$F_{UU,\mathcal{P}}^\Phi = \frac{1}{4\,(4\pi)^3}z\sum_n\sum_a\int_{x_B}^{\hat{x}_{\max}}\frac{\mathrm{d}\hat{x}}{\hat{x}}\int_z^1\frac{\mathrm{d}\hat{z}}{\hat{z}}\frac{1}{Q^2}f_1^a(\xi;\mu^2)\epsilon_{\mathcal{P};\Phi}^{\mu\nu}H_\mu^{(a)[n]}H_\nu^{(a)[n]*}\langle\mathcal{O}[n]\rangle$$
$$\times \delta\left(\frac{(1-\hat{x})(1-\hat{z})}{\hat{x}\hat{z}} - \frac{1-\hat{z}}{\hat{z}^2}\frac{M_\psi^2}{Q^2} - \frac{\boldsymbol{q}_T^2}{Q^2}\right)\delta(z-\hat{z}), \tag{2.12}$$

where the sum n runs over the dominant LDMEs $\langle\mathcal{O}[n]\rangle$ and a runs over the parton types. Furthermore, we introduced the partonic scaling variables

$$\hat{x} = \frac{Q^2}{2p_a\cdot q} = \frac{x_B}{\xi}, \quad \hat{z} = \frac{p_a\cdot P_\psi}{p_a\cdot q} = z, \tag{2.13}$$

together with

$$\hat{x}_{\max} = \frac{Q^2}{M_\psi^2 + Q^2} \ . \tag{2.14}$$

In ref. [16] the Dirac delta present in eq. (2.12) was expanded at small-$\boldsymbol{q}_T$ as follows (see its appendix B for the derivation)

$$\delta\left(\frac{(1-\hat{x})(1-\hat{z})}{\hat{x}\hat{z}} - \frac{1-\hat{z}}{\hat{z}^2}\frac{M_\psi^2}{Q^2} - \frac{\boldsymbol{q}_T^2}{Q^2}\right) \sim \hat{x}_{\max}\left[\log\frac{M_\psi^2 + Q^2}{\boldsymbol{q}_T^2}\delta(1-\hat{x}')\delta(1-\hat{z})\right.$$
$$\left. + \frac{\hat{x}'}{(1-\hat{x}')_+}\delta(1-\hat{z}) + \frac{M_\psi^2 + Q^2}{M_\psi^2/\hat{z} + Q^2}\frac{\hat{z}}{(1-\hat{z})_+}\delta(1-\hat{x}')\right], \tag{2.15}$$

where

$$\hat{x}' = \frac{\hat{x}}{\hat{x}_{\max}} \ . \tag{2.16}$$

Note that on the right-hand side of eq. (2.15) the coefficient in front of the double delta logarithmically diverges with $\boldsymbol{q}_T$. However, as we have found this is not sufficient to obtain the correct behavior of structure functions in the ITM region, which is restored by adding a constant term to the double-delta coefficient.[1] The need to include this subdominant term can also be understood from the following argument. The Dirac-delta expansion in eq. (2.15) was obtained in ref. [16] by applying the full Dirac delta to two continuous test functions. However, the structure functions defined in eq. (2.12) contain discontinuities that come from the soft gluon radiation associated with the CO final state in the NRQCD calculations (see appendix B). These contributions are made explicit via the decomposition into poles through a Laurent expansion, namely[2]

$$\frac{1}{(4\pi)^3} \frac{1}{Q^2} \epsilon_{\mathcal{P};\Phi}^{\mu\nu} H_\mu^{(a)[n]} H_\nu^{(a)[n]*} \equiv \mathcal{H}_{\mathcal{P};\Phi}^{(a)[n]}(\hat{x}',\hat{z}) = \mathcal{H}_{\mathcal{P};\Phi}^{(a)[n];(0)}(\hat{x}',\hat{z}) + \sum_{k=1}^\infty \left(\frac{1-\hat{z}}{1-\hat{x}'}\right)^k \mathcal{H}_{\mathcal{P};\Phi}^{(a)[n];(k)}(\hat{z}), \tag{2.17}$$

where $\mathcal{H}_{\mathcal{P};\Phi}^{(a)[n];(0)}$ and all $\mathcal{H}_{\mathcal{P};\Phi}^{(a)[n];(k)}$ are finite. Despite the different notation, the amplitude squared on the left-hand side of eq. (2.17) is in agreement with refs. [24, 25]. Note that to get the pole structure on the right-hand side of eq. (2.17) we are explicitly writing the amplitude squared in terms of $\hat{x}'$ and $\hat{z}$ (eqs. (2.13) and (2.16)). We have found that for J/ψ production in SIDIS the poles are present only for the gluon-initiated process $\gamma^* g$ with the expansion running up to $k = 2$. Instead, the quark-initiated processes $\gamma^* q$ are fully described by the $k = 0$ finite term. Moreover, up to the precision considered in this work, the poles contribute only to the structure functions $F_{UU,\mathcal{P}}$ introduced in eq. (2.4).

These poles are under control when the amplitude squared is evaluated at high-$\boldsymbol{q}_T$ values, as the transverse momentum forces the phase space to deviate from $\hat{z} = 1$ and $\hat{x}' = 1$. Solely when we consider the small-$\boldsymbol{q}_T$ limit they have a significant impact. The Dirac-delta expansion in eq. (2.15) is applicable only to the first term ($\mathcal{H}_{\mathcal{P},\Phi}^{(a)[n];(0)}$), while all the others require a different approach. In particular, we can split the differential cross section in eq. (2.4) into three parts in the HTM region, namely

$$\frac{\mathrm{d}\sigma}{\mathrm{d}x_B \mathrm{d}y \mathrm{d}z \mathrm{d}\boldsymbol{q}_T^2 \mathrm{d}\phi_\psi} \equiv \mathrm{d}\sigma_A + \mathrm{d}\sigma_B + \mathrm{d}\sigma_C, \tag{2.18}$$

---

[1]Note that this new term has the same divergence order as the other terms on right-hand side of eq. (2.15), namely the coefficients of $\delta(1 - \hat{x}')$ and $\delta(1 - \hat{z})$.

[2]Before performing the expansion, we suggest applying once the following relation, obtained from the Dirac delta:

$$\frac{1}{1-\hat{z}} = \frac{(\hat{z} - \hat{x}')M_\psi^2 + \hat{z}(1-\hat{x}')Q^2}{\hat{x}'\hat{z}^2\boldsymbol{q}_T^2} \ .$$

with

$$
\begin{aligned}
\mathrm{d}\sigma_A = {} & \frac{\alpha}{4yQ^2} z \sum_n \int_0^1 \mathrm{d}\hat{x}' \int_0^1 \mathrm{d}\hat{z}\, f_1^a\!\left(\frac{x_B}{\hat{x}_{\max}\hat{x}'};\mu^2\right)\hat{z}\;\delta(G(\hat{x}',\hat{z}))\delta(z-\hat{z}) \\
& \times \Bigg\{ \left[1+(1-y)^2\right]\mathcal{H}_\perp^{(a)[n];(0)}(\hat{x}',\hat{z}) + 4(1-y)\mathcal{H}_\parallel^{(a)[n];(0)}(\hat{x}',\hat{z}) \\
& + 2(2-y)\sqrt{1-y}\cos\phi_\psi \mathcal{H}_{\cos\phi_\psi}^{(a)[n];(0)}(\hat{x}',\hat{z}) + 4(1-y)\cos2\phi_\psi \mathcal{H}_{\cos2\phi_\psi}^{(a)[n];(0)}(\hat{x}',\hat{z}) \Bigg\}\langle\mathcal{O}[n]\rangle\;, \\
\mathrm{d}\sigma_B = {} & \frac{\alpha}{4yQ^2} z \sum_n \int_0^1 \mathrm{d}\hat{x}' \int_0^1 \mathrm{d}\hat{z}\, f_1^g\!\left(\frac{x_B}{\hat{x}_{\max}\hat{x}'};\mu^2\right)\hat{z}\;\delta(G(\hat{x}',\hat{z}))\delta(z-\hat{z}) \\
& \times \left(\frac{1-\hat{z}}{1-\hat{x}'}\right)\left[\left(1+(1-y)^2\right)\mathcal{H}_\perp^{(g)[n];(1)}(\hat{z}) + 4(1-y)\mathcal{H}_\parallel^{(g)[n];(1)}(\hat{z})\right]\langle\mathcal{O}[n]\rangle, \\
\mathrm{d}\sigma_C = {} & \frac{\alpha}{4yQ^2} z \sum_n \int_0^1 \mathrm{d}\hat{x}' \int_0^1 \mathrm{d}\hat{z}\, f_1^g\!\left(\frac{x_B}{\hat{x}_{\max}\hat{x}'};\mu^2\right)\hat{z}\;\delta(G(\hat{x}',\hat{z}))\delta(z-\hat{z}) \\
& \times \left(\frac{1-\hat{z}}{1-\hat{x}'}\right)^2\left[\left(1+(1-y)^2\right)\mathcal{H}_\perp^{(g)[n];(2)}(\hat{z}) + 4(1-y)\mathcal{H}_\parallel^{(g)[n];(2)}(\hat{z})\right]\langle\mathcal{O}[n]\rangle,
\end{aligned}
\tag{2.19}
$$

where the function $G(\hat{x}',\hat{z})$ is given by

$$
G(\hat{x}',\hat{z}) = \hat{z}(1-\hat{z})(1-\hat{x}') - \frac{M_\psi^2}{Q^2}(1-\hat{z})(\hat{x}'-\hat{z}) - \frac{\boldsymbol{q}_T^2}{Q^2}\hat{x}'\hat{z}^2.
\tag{2.20}
$$

The difference in the lower integration limit for both $\hat{x}'$ and $\hat{z}$ between eqs. (2.12) and (2.19) has been introduced for the convenience of the calculation. This modification is possible since the added integration range does not contribute to the final result (see appendix A of this work and appendix B of [16]). As mentioned, one can apply directly the delta expansion in eq. (2.15) to evaluate the small-$\boldsymbol{q}_T$ behavior of $\mathrm{d}\sigma_A$. Instead, the expansions of $\mathrm{d}\sigma_B$ and $\mathrm{d}\sigma_C$ are obtained by considering the integral w.r.t. $\mathrm{d}\hat{x}$ and $\mathrm{d}\hat{z}$ of those terms that are truly indeterminate in the limit $\boldsymbol{q}_T \to 0$, with the indeterminacy solved by the presence of the full Dirac delta (see eq. (2.20)).

Therefore, it is legitimate to approximate $\mathcal{H}_{\mathcal{P}}^{[n];(k)}(\hat{z}) \to \mathcal{H}_{\mathcal{P}}^{[n];(k)}(1)$ which gives

$$
\begin{aligned}
\mathcal{H}_{\mathcal{P}}^{(g)[n];(1)}(1) &= -2\frac{M_\psi^2}{M_\psi^2 + Q^2}\mathcal{H}_{\mathcal{P}}^{(g)[n];(0)}(1,1), \\
\mathcal{H}_{\mathcal{P}}^{(g)[n];(2)}(1) &= \left(\frac{M_\psi^2}{M_\psi^2 + Q^2}\right)^2 \mathcal{H}_{\mathcal{P}}^{(g)[n];(0)}(1,1)\;.
\end{aligned}
\tag{2.21}
$$

Hence from eq. (2.19) we obtain

$$
\begin{aligned}
\mathrm{d}\sigma_B \approx {} & \frac{\alpha}{4yQ^2} f_1^g(x;\mu^2)\left(-\hat{x}_{\max}\log\frac{M_\psi^2}{\boldsymbol{q}_T^2}\right) \\
& \times \sum_n \left[\left(1+(1-y)^2\right)\mathcal{H}_\perp^{(g)[n];(0)}(1,1) + 4(1-y)\mathcal{H}_\parallel^{(g)[n];(0)}(1,1)\right]\langle\mathcal{O}[n]\rangle\delta(1-z)
\end{aligned}
\tag{2.22}
$$

and

$$d\sigma_C \approx \frac{\alpha}{4yQ^2} f_1^g(x;\mu^2) \left[\frac{\hat{x}_{\max}}{2} \left(\log \frac{M_\psi^2}{\boldsymbol{q}_T^2} - 1 \right) \right]$$
$$\times \sum_n \left[\left(1 + (1-y)^2 \right) \mathcal{H}_\perp^{(g)[n];(0)}(1,1) + 4(1-y)\mathcal{H}_\parallel^{(g)[n];(0)}(1,1) \right] \langle \mathcal{O}[n] \rangle \delta(1-z), \tag{2.23}$$

where $x \equiv x_B/\hat{x}_{\max}$. More details on the previous results can be found in appendix A. Since the small-$\boldsymbol{q}_T$ limit of these quantities is proportional to $\mathcal{H}^{[n];(0)}(1,1)$, we can effectively add these terms to the double delta coefficient, obtaining that

$$\mathcal{H}_\mathcal{P}^{(g)[n]}(\hat{x}',\hat{z})\delta\left(\frac{G(\hat{x}',\hat{z})}{\hat{x}'\hat{z}^2} \right) \sim \mathcal{H}_\mathcal{P}^{(g)[n];(0)}(\hat{x}',\hat{z}) \; \delta_{\text{eff}}(\hat{x}',\hat{z}), \tag{2.24}$$

with

$$\delta_{\text{eff}}(\hat{x}',\hat{z}) = \hat{x}_{\max} \left[\frac{1}{2} \left(\log \frac{M_\psi^2 + Q^2}{\boldsymbol{q}_T^2} - 1 - \log \frac{M_\psi^2}{M_\psi^2 + Q^2} \right) \delta(1-\hat{x}')\delta(1-\hat{z}) \right.$$
$$\left. + \frac{\hat{x}'}{(1-\hat{x}')_+}\delta(1-\hat{z}) + \frac{M_\psi^2 + Q^2}{M_\psi^2/\hat{z} + Q^2} \frac{\hat{z}}{(1-\hat{z})_+}\delta(1-\hat{x}') \right]. \tag{2.25}$$

Considering the contributions from the various terms in eq. (2.25), we found that the small-$\boldsymbol{q}_T$ limit is dominated by the first two terms for this $\gamma^* g$ channel (and similarly the first two terms of eq. (2.15) for the quark and antiquark channels). Instead, the contribution coming from the "+"-distribution of $\hat{z}$ is subdominant and can be neglected in the following. In principle, this last term will lead to a fragmentation-like contribution to the process considered here. We will further comment on the connection to a fragmentation description below.

Hence, the leading power behavior of the structure functions in the ITM region is given by

$$F_{UU,\mathcal{P}} = \sigma_{UU,\mathcal{P}} \frac{\alpha_s}{\boldsymbol{q}_T^2} \Big[L(\boldsymbol{q}_T^2)f_1^g(x;\mu^2) + \left(P_{gg} \otimes f_1^g + P_{gi} \otimes f_1^i \right)(x;\mu^2) \Big],$$
$$F_{UU}^{\cos 2\phi_\psi} = \sigma_{UU}^{\cos 2\phi_\psi} \frac{\alpha_s}{\boldsymbol{q}_T^2} \left(\delta P_{gg} \otimes f_1^g + \delta P_{gi} \otimes f_1^i \right)(x;\mu^2), \tag{2.26}$$

while $F_{UU}^{\cos\phi_\psi}$ is suppressed by a factor of $|\boldsymbol{q}_T|/\mu_H$ w.r.t. the other structure functions. This is in accordance with the TMD formula in eq. (2.5) which does not show any $\cos\phi_\psi$ contribution too. The logarithmic function $L(\boldsymbol{q}_T^2)$ reads

$$L(\boldsymbol{q}_T^2) = C_A \left(\log \frac{M_\psi^2 + Q^2}{\boldsymbol{q}_T^2} - 1 - \log \frac{M_\psi^2}{M_\psi^2 + Q^2} - \frac{11 - 4n_f T_R/C_A}{6} \right), \tag{2.27}$$

and the quantities $\sigma_{UU,\mathcal{P}}$ and $\sigma_{UU}^{\cos 2\phi_\psi}$ are related to the partonic process $\gamma^* g \to c\bar{c}[n]$ and they correspond to (see ref. [16])

$$\sigma_{UU,\perp} = \frac{e_c^2 \alpha \alpha_s}{M_\psi \left(M_\psi^2 + Q^2\right)} \left[\langle \mathcal{O}[^1S_0^{[8]}] \rangle + 4 \frac{7M_\psi^4 + 2M_\psi^2 Q^2 + 3Q^4}{M_\psi^2 \left(M_\psi^2 + Q^2\right)^2} \langle \mathcal{O}[^3P_0^{[8]}] \rangle \right] \delta(1-z),$$

$$\sigma_{UU,\parallel} = \frac{e_c^2 \alpha \alpha_s}{M_\psi \left(M_\psi^2 + Q^2\right)} \left[16 \frac{Q^2}{\left(M_\psi^2 + Q^2\right)^2} \langle \mathcal{O}[^3P_0^{[8]}] \rangle \right] \delta(1-z),$$

$$\sigma_{UU}^{\cos 2\phi_\psi} = \frac{e_c^2 \alpha \alpha_s}{M_\psi \left(M_\psi^2 + Q^2\right)} \left[-\langle \mathcal{O}[^1S_0^{[8]}] \rangle + 4 \frac{3M_\psi^2 - Q^2}{M_\psi^2 \left(M_\psi^2 + Q^2\right)} \langle \mathcal{O}[^3P_0^{[8]}] \rangle \right] \delta(1-z) .$$

$$(2.28)$$

Moreover, P_{ab} in eq. (2.26) denotes the leading order, fully unpolarized splitting functions, that can be found in ref. [26], while δP_{ab} are the splitting function of an unpolarized parton into a linearly polarized gluon, which can be found in refs. [27, 28]. The convolution (denoted by the "$\otimes$" symbol) between these splitting functions and the parton distribution functions is defined as

$$(\mathcal{P} \otimes f_1^a)(x; \mu^2) = \int_x^1 \frac{\mathrm{d}\hat{x}'}{\hat{x}'} \mathcal{P}_{ab}(\hat{x}'; \mu^2) f_1^b(x/\hat{x}'; \mu^2), \qquad (2.29)$$

where $\mathcal{P}_{ab}$ denotes either P_{ab} or δP_{ab}.

The logarithmic function defined in eq. (2.27) is our most important difference compared to ref. [16], where the logarithmic function contains twice the logarithm $\log[(M_\psi^2 + Q^2)/\boldsymbol{q}_T^2]$ compared to eq. (2.27). This is due to the presence of the poles, not considered in ref. [16]. Indeed, it is through the inclusion of eqs. (2.22) and (2.23) that in eq. (2.27) one of the logarithms has been removed. The price to pay corresponds to the novel $\boldsymbol{q}_T$-independent terms found, namely $1 + \log[(M_\psi^2 + Q^2)/M_\psi^2]$. Clearly, eq. (2.27) has an impact on the TMDShF derivation too, as will be discussed in section 2.2. Besides, eq. (2.27) implies the presence of divergences related to soft gluon emission from the leading order $\gamma^* g \to c\bar{c}[n]$ process. It is then possible to check the validity of this expression by investigating the soft-limit of eq. (2.6) via the eikonal method, as done in appendix B.

Although our work is based on the J/ψ production in SIDIS, we expect that the presence of the poles as in eq. (2.17) is an intrinsic feature of any inclusive quarkonium production, and they apply to different processes and observables too. Hence, the suppression of the $\boldsymbol{q}_T$-logarithm in eq. (2.27) is not an exclusive outcome of the specific process under consideration, but rather a general statement. Thus, these discontinuities may be connected to other regularization procedures associated with CO contributions to heavy quarkonium productions. While it is worthwhile to further pursue these connections in the NRQCD factorization, we consider such a study to be beyond the scope of the current paper but we hope to address it in the future. However, to emphasize the importance of further investigation, we will briefly comment on the similarities of our findings with those obtained by adopting the fragmentation function description.

The same cross section in the HTM region can be expressed in terms of fragmentation functions, as shown in refs. [29–31]. Hence, the TMDShF may also be seen as a

fragmentation-like function of a $c\bar{c}$ into a J/ψ evaluated at ITM. The evolution of the latter has been studied in ref. [30], which includes real contributions having a component proportional to the $(1 - \hat{z})_+$ distribution and another one to $\delta(1 - \hat{z})$. Hence, our analysis is related to the latter term. However, an important difference concerns the integration range of the outgoing gluon. The integration of the soft-gluon momentum in our case has a lower limit set by the J/ψ transverse momentum (see eq. (B.11) of appendix B), whereas no lower limit is present in ref. [30] causing infrared divergences. Therefore, the connection between our work and the fragmentation-function description cannot be carried out further without the inclusion of next order (real and virtual) contributions and, as previously stated, we leave this discussion to further studies.

2.2 From low to intermediate transverse momentum

In this section we evaluate the evolution of the structure functions valid in the LTM region ($|\boldsymbol{q}_T| \ll \mu_H$) up to the ITM region. Even if not formally proven, there are strong arguments in favor of TMD factorization [12]. Therefore, the differential cross section for the semi-inclusive production of a J/ψ with a small transverse momentum component is given by eq. (2.5). In this case, the structure functions $\mathcal{F}$ can be calculated from the partonic process

$$\gamma^*(q) + g(p_a) \to c\bar{c}[n](P_\psi), \tag{2.30}$$

where, contrarily to the HTM case, the initial gluon has a non-negligible transverse momentum component w.r.t. the parent proton, namely

$$p_a^\mu = \xi P^\mu + p_T^\mu, \tag{2.31}$$

with $p_T^2 = -\boldsymbol{p}_T^2$. Hence, eq. (2.30) leads to

$$\mathcal{F}_{UU,\perp} = 2\pi^2 \frac{e_c^2 \alpha \alpha_s}{M_\psi \left(M_\psi^2 + Q^2\right)} \left(\mathcal{C}\left[f_1^g \Delta^{[^1S_0^{[8]}]}\right] + 4\frac{7M_\psi^4 + 2M_\psi^2 Q^2 + 3Q^4}{M_\psi^2 \left(M_\psi^2 + Q^2\right)^2} \mathcal{C}\left[f_1^g \Delta^{[^3P_0^{[8]}]}\right] \right),$$

$$\mathcal{F}_{UU,\parallel} = 2\pi^2 \frac{e_c^2 \alpha \alpha_s}{M_\psi \left(M_\psi^2 + Q^2\right)} \left(16\frac{Q^2}{\left(M_\psi^2 + Q^2\right)^2} \mathcal{C}\left[f_1^g \Delta^{[^3P_0^{[8]}]}\right] \right),$$

$$\mathcal{F}_{UU}^{\cos 2\phi_\psi} = \frac{\pi^2}{2} \frac{e_c^2 \alpha \alpha_s}{M_\psi \left(M_\psi^2 + Q^2\right)} \left(-\mathcal{C}\left[wh_1^{\perp g} \Delta_h^{[^1S_0^{[8]}]}\right] + 4\frac{3M_\psi^2 - Q^2}{M_\psi^2 \left(M_\psi^2 + Q^2\right)} \mathcal{C}\left[wh_1^{\perp g} \Delta_h^{[^3P_0^{[8]}]}\right] \right).$$
$$\tag{2.32}$$

Following refs. [14–17, 22], we consider from the beginning the TMD factorized formula that includes the presence of a TMDShF, $\Delta^{[n]}$ or $\Delta_h^{[n]}$, which is related to the production of a J/ψ with a small transverse momentum component w.r.t. the photon and proton. As commented below eq. (2.25), in this paper we focus on the $\delta(1 - \hat{z})$ contribution from the TMDShF. Subdominant terms and higher order corrections are also expected to contribute away from $z = 1$. In that case the description of the heavy quark pair that hadronizes into the heavy quarkonium state will be even more similar to a single-parton TMD fragmentation functions description applied in light hadron production. See also ref. [32] for a description involving both single parton and parton-pair fragmentation processes.

In the above equations convolutions between the TMD distributions and the TMDShFs appear, namely

$$\mathcal{C}\left[f_1^g \Delta^{[n]}\right](x, z, \boldsymbol{q}_T^2) = \int \mathrm{d}^2\boldsymbol{p}_T \int \mathrm{d}^2\boldsymbol{k}_T \delta^2(\boldsymbol{p}_T + \boldsymbol{k}_T - \boldsymbol{q}_T) f_1^g(x, \boldsymbol{p}_T^2) \Delta^{[n]}(z, \boldsymbol{k}_T^2),$$

$$\mathcal{C}\left[w h_1^{\perp g} \Delta_h^{[n]}\right](x, z, \boldsymbol{q}_T^2) = \int \mathrm{d}^2\boldsymbol{p}_T \int \mathrm{d}^2\boldsymbol{k}_T \delta^2(\boldsymbol{p}_T + \boldsymbol{k}_T - \boldsymbol{q}_T) w(\boldsymbol{p}_T, \boldsymbol{k}_T) h_1^{\perp g}(x, \boldsymbol{p}_T^2) \Delta_h^{[n]}(z, \boldsymbol{k}_T^2),$$

$$\tag{2.33}$$

where in the last line we introduced the weight function w defined as (with M_p the proton mass)

$$w(\boldsymbol{p}_T, \boldsymbol{k}_T) = \frac{1}{M_p^2 \left(\boldsymbol{p}_T + \boldsymbol{k}_T\right)^2}\left[2(\boldsymbol{p}_T \cdot \boldsymbol{k}_T)^2 + \boldsymbol{p}_T^2\left(\boldsymbol{p}_T^2 - \boldsymbol{k}_T^2\right)\right]. \tag{2.34}$$

Beyond the parton model approximation, soft gluon radiation to all orders is included into an exponential Sudakov factor. One can relate its logarithmic divergences to the TMD objects (both PDFs and shape function) involved in the reactions, whereas the remaining perturbative q_T-independent corrections are collected into the hard term. As a consequence of the regularization of their ultraviolet and rapidity divergences, TMD-PDFs depend on two different scales, respectively μ and $\sqrt{\zeta}$. We take these two scales to be equal and denote them by μ. In contrast, there are no rapidity divergences associated to the TMDShF. Thus, we can impose for its rapidity parameter $\zeta_\Delta = 1$, in line with ref. [33].

Implementing TMD evolution is more easily done in impact parameter space, where convolutions in the cross section become simple products. Besides, in ref. [16] it was found that, up to the precision considered, from the matching procedure it is possible to deduce only the naive order-α_s^0 part of $\Delta_h^{[n]}(z, \boldsymbol{k}_T^2)$ that is proportional to $\delta(\boldsymbol{k}_T^2)$. Note that in reality smearing effects will be involved, but that small-$\boldsymbol{k}_T$ behavior cannot be obtained from a perturbative matching calculation, at least up to the perturbative order considered here. As a consequence, in the following we focus on the convolution $\mathcal{C}[f_1^g \Delta^{[n]}]$.

We define the Fourier transform of $f_1^a(x, \boldsymbol{p}_T^2)$ as

$$\widetilde{f}_1^a(x, \boldsymbol{b}_T^2) = \frac{1}{2\pi} \int \mathrm{d}^2\boldsymbol{p}_T \mathrm{e}^{i\boldsymbol{b}_T \cdot \boldsymbol{p}_T} f_1^a(x, \boldsymbol{p}_T^2), \tag{2.35}$$

and the Fourier transformed TMDShF as

$$\widetilde{\Delta}^{[n]}(z, \boldsymbol{b}_T^2) = \frac{1}{2\pi} \int \mathrm{d}^2\boldsymbol{k}_T \mathrm{e}^{i\boldsymbol{b}_T \cdot \boldsymbol{k}_T} \Delta^{[n]}(z, \boldsymbol{k}_T^2), \tag{2.36}$$

from which

$$\mathcal{C}[f_1^g \Delta^{[n]}](x, z, \boldsymbol{q}_T^2; \mu^2 = \mu_H^2) = \int \mathrm{d}^2\boldsymbol{b}_T \mathrm{e}^{-i\boldsymbol{b}_T \cdot \boldsymbol{q}_T} \widetilde{f}_1^g(x, \boldsymbol{b}_T^2; \mu_H^2) \widetilde{\Delta}^{[n]}(z, \boldsymbol{b}_T^2; \mu_H^2), \tag{2.37}$$

where we fixed the factorization scale so that the convolutions are evaluated at the hard scale. The perturbative tail of the fully unpolarized gluon TMD f_1^g, valid in the limit $|\boldsymbol{b}_T| \ll 1/\Lambda_{\mathrm{QCD}}$, is given by [26]

$$\widetilde{f}_1^g(x, \boldsymbol{b}_T^2; \mu_H^2) = \frac{1}{2\pi} \sum_{a=q,\bar{q},g} (C_{g/a} \otimes f_1^a)(x; \mu_b^2) \mathrm{e}^{-\frac{1}{2} S_A^g(\boldsymbol{b}_T^2; \mu_H^2)}, \tag{2.38}$$

where $\mu_b = b_0/|\boldsymbol{b}_T|$ with $b_0 = 2\mathrm{e}^{-\gamma_E} \approx 1.123$. Note that the coefficient function $C_{a/b}$ in eq. (2.38) can be expanded in powers of α_s

$$C_{g/a}(x, \mu_b^2) = \delta_{ab}\delta(1-x) + \sum_{k=1}^{\infty} C_{g/a}^{(k)}(x)\left(\frac{\alpha_s(\mu_b)}{\pi}\right)^k, \qquad (2.39)$$

and can be explicitly found in refs. [26, 34]. Nevertheless, the coefficient $C_{g/a}^{(k)}$ in the right-hand side of eq. (2.39) will not enter in the following (leading order) discussion since they are independent of the parameter b_T. Consequently, their explicit expression at all orders is not required. Furthermore, the (leading order) Sudakov factor S_A present in eq. (2.38) reads

$$\begin{aligned}
S_A^g(\boldsymbol{b}_T^2; \mu_H^2) &= \frac{C_A}{\pi} \int_{\mu_b^2}^{\mu_H^2} \frac{\mathrm{d}\mu'^2}{\mu'^2} \alpha_s(\mu')\left[\log\frac{\mu^2}{\mu'^2} - \frac{11 - 4n_f T_R/C_A}{6}\right] \\
&= \frac{C_A}{\pi}\alpha_s\left(\frac{1}{2}\log^2\frac{\mu_H^2}{\mu_b^2} - \frac{11 - 4n_f T_R/C_A}{6}\log\frac{\mu_H^2}{\mu_b^2}\right),
\end{aligned} \qquad (2.40)$$

where in the last line the running of the coupling has been neglected. By inserting eqs. (2.39) and (2.40) in eq. (2.38) and using the DGLAP equations to evolve the PDF from a scale μ_H down to the scale $\mu_b < \mu_H$, we find that up to order α_s the perturbative tail of the gluon TMD-PDF reads [34]

$$\begin{aligned}
\widetilde{f}_1^g(x, \boldsymbol{b}_T^2; \mu_H^2) &= \frac{1}{2\pi}\bigg\{f_1^g(x; \mu_H^2) - \frac{\alpha_s}{2\pi}\bigg[C_A\bigg(\frac{1}{2}\log^2\frac{\mu_H^2}{\mu_b^2} - \frac{11 - 4n_f T_R/C_A}{6}\log\frac{\mu_H^2}{\mu_b^2}\bigg)f_1^g(x; \mu_H^2) \\
&\quad + \left(P_{gg} \otimes f_1^g + P_{gi} \otimes f_1^i\right)(x; \mu_H^2)\log\frac{\mu_H^2}{\mu_b^2} - 2\sum_{a=q,\bar{q},g}(C_{g/a}^{(1)} \otimes f_1^a)(x; \mu_H^2)\bigg]\bigg\},
\end{aligned} \qquad (2.41)$$

where once again P_{ab} denotes the leading order splitting functions [26]. Employing this, and by requiring that the TMD expressions evolved to the scale $\mu_H^2 \equiv \widetilde{Q}^2 = M_\psi^2 + Q^2$ match with the expansion of the collinear ones obtained in eq. (2.26), we deduce the TMDShF perturbative tail

$$\begin{aligned}
\widetilde{\Delta}^{[n]}(z, \boldsymbol{b}_T^2; \mu^2 = \widetilde{Q}^2) &= \frac{1}{2\pi}\left[1 + \frac{\alpha_s}{2\pi}C_A\left(1 + \log\frac{M_\psi^2}{M_\psi^2 + Q^2}\right)\log\frac{\widetilde{Q}^2}{\mu_b^2}\right]\langle\mathcal{O}[n]\rangle\delta(1-z) \\
&\quad + \mathcal{O}(\alpha_s^2) + \mathcal{O}(b_T\Lambda_{\mathrm{QCD}}),
\end{aligned} \qquad (2.42)$$

which in momentum space becomes

$$\Delta^{[n]}(z, \boldsymbol{k}_T^2; \widetilde{Q}^2) = -\frac{\alpha_s}{2\pi^2 \boldsymbol{k}_T^2}C_A\left(1 + \log\frac{M_\psi^2}{M_\psi^2 + Q^2}\right)\langle\mathcal{O}[n]\rangle\delta(1-z), \qquad (2.43)$$

valid in the $|\boldsymbol{k}_T| \gg \Lambda_{\mathrm{QCD}}$ limit. Inserting eq. (2.42) in eq. (2.37), we find that the convolution in momentum space is given by

$$\begin{aligned}
&\mathcal{C}[f_1^g \Delta^{[n]}](x, z, \boldsymbol{q}_T^2; \widetilde{Q}^2) \\
&\quad = \frac{\alpha_s}{2\pi^2 \boldsymbol{q}_T^2}\left[L(\boldsymbol{q}_T^2)f_1^g(x; \widetilde{Q}^2) + (P_{gg} \otimes f_1^g + P_{gi} \otimes f_1^i)(x; \widetilde{Q}^2)\right]\langle\mathcal{O}[n]\rangle\delta(1-z),
\end{aligned} \qquad (2.44)$$

where $L(\boldsymbol{q}_T^2)$ is the logarithmic function defined in eq. (2.27). Hence, with the choice $\mu = \widetilde{Q}$, the first two lines of eq. (2.32) and the first line of eq. (2.26) match. Note how the modification of eq. (2.27) compared to ref. [16] has a significant impact on the TMDShF expression. Indeed, the TMDShF perturbative tail in eq. (2.43) does not contain any kind of logarithmic divergence in $\boldsymbol{k}_T$, being tamed by the presence of the heavy mass. We emphasized that the absence of $\boldsymbol{k}_T$-divergent terms associated to the quarkonium is in accordance with other works in the literature, e.g. refs. [14, 15, 18–21].

For completeness, we remark that the matching of $F_{UU}^{\cos 2\phi_\psi}$ and $\mathcal{F}_{UU}^{\cos 2\phi_\psi}$, which involves the second convolution in eq. (2.33), is fulfilled by taking the perturbative tail of $h_1^{\perp g}$ [27] up to α_s order

$$h_1^{\perp g}(x, \boldsymbol{p}_T^2) = \frac{\alpha_s}{\pi^2} \frac{2M_p^2}{\boldsymbol{p}_T^4} (\delta P_{gg} \otimes f_1^g + \delta P_{gi} \otimes f_1^i)(x) + \mathcal{O}(\alpha_s^2) \tag{2.45}$$

and the leading order naive shape function

$$\Delta_h^{[n]}(z, \boldsymbol{k}_T^2) = \delta(\boldsymbol{k}_T^2)\langle \mathcal{O}[n]\rangle \delta(1-z) + \mathcal{O}(\alpha_s), \tag{2.46}$$

from which

$$\mathcal{C}[wh_1^{\perp g}\Delta_h^{[n]}](x, z, \boldsymbol{q}_T^2; \mu^2) = \frac{2}{\pi^2} \frac{\alpha_s}{\boldsymbol{q}_T^2} (\delta P_{gg} \otimes f_1^g + \delta P_{gi} \otimes f_1^i)(x; \mu^2)\langle \mathcal{O}[n]\rangle \delta(1-z) . \tag{2.47}$$

Since the $h_1^{\perp g}$ expansion starts at order α_s, we notice that to get the non-trivial perturbative tail of Δ_h it is required that the SIDIS cross section within NRQCD is evaluated at order $\alpha\alpha_s^3$. However, this calculation is currently unavailable.

3 Universality

In the previous section, we found that an extra factor Δ is needed to absorb all the $\boldsymbol{q}_T$-divergent terms coming from the collinear limit, and we identified it as the dominant TMDShF perturbative tail. However, it has been obtained at the particular scale $\widetilde{Q}$, whereas for more general application it needs to be considered at a general scale μ_H. This can be obtained by tracing back the μ_H dependence in eq. (2.27), that is related to the full Sudakov factor for J/ψ production in SIDIS in terms of this general scale and up to order α_s, namely

$$S_A^{ep,\psi}(\boldsymbol{b}_T^2; \mu_H^2) = \frac{1}{2}S_A^g(\boldsymbol{b}_T^2; \mu_H^2) + B_{ep}(\mu_H^2)\log\frac{\mu_H^2}{\mu_b^2}, \tag{3.1}$$

where

$$B_{ep}(\mu_H^2) = -\frac{\alpha_s}{2\pi}C_A\left(1 + \log\frac{M_\psi^2\mu_H^2}{(M_\psi^2 + Q^2)^2}\right) . \tag{3.2}$$

We checked that eq. (3.1) (and subsequently eq. (3.2)) agrees in the kinematic limit corresponding to a bound pair with the Sudakov factor obtained in the open heavy-quark pair production in electron-proton collisions, which can be found in ref. [19].

It is not natural to fully include eq. (3.2) into something that we identify as the TMDShF. Indeed, being a quarkonium-related object, its complete dependence is given by

$\Delta_{\mathrm{ShF}}^{[n]}(z, \boldsymbol{k}_T^2; M_\psi^2, \mu^2 = \mu_H^2)$, while it may depend on the process-related hard-quantity Q only via the μ_H choice. Thus, the Q^2 dependence deriving from eq. (3.2) must stem from a process dependent part, which can be incorporated into an extra process-dependent factor $S(\boldsymbol{b}_T^2; M_\psi^2, Q^2, \mu^2 = \mu_H^2)$.

Therefore, we split the full $\Delta_{ep}^{[n]}$ into these two terms:[3]

$$\Delta_{ep}^{[n]}(\mu_H^2) = \Delta_{\mathrm{ShF}}^{[n]}(\mu_H^2) \times S_{ep}(\mu_H^2) . \tag{3.3}$$

The $\Delta_{\mathrm{ShF}}^{[n]}$ is what we truly identify as the TMDShF and is universal because it solely depends on M_ψ. Instead, the S_{ep} is an extra soft factor which incorporates the specific process dependence and it can be removed by a proper choice of the factorization scale $\mu = \mu_H$. This implies that at that scale the full $\Delta_{ep}^{[n]}$ is equivalent to the TMDShF. At this level, the simplest way to perform the splitting in b_T-space is to take

$$\widetilde{\Delta}_{\mathrm{ShF}}^{[n]}(z, \boldsymbol{b}_T^2; \mu_H^2) = \frac{1}{2\pi} \left[1 + \frac{\alpha_s}{2\pi} C_A \left(1 + \log \frac{M_\psi^2}{\mu_H^2} \right) \log \frac{\mu_H^2}{\mu_b^2} \right] \langle \mathcal{O}[n] \rangle \delta(1 - z), \tag{3.4}$$

$$S_{ep}(\boldsymbol{b}_T^2; \mu_H^2) = 1 + \frac{\alpha_s}{2\pi} C_A \left(2 \log \frac{\mu_H^2}{M_\psi^2 + Q^2} \right) \log \frac{\mu_H^2}{\mu_b^2} . \tag{3.5}$$

With this splitting convention and by taking $\mu_H \equiv \widetilde{Q}$, the full $\Delta_{ep}^{[n]}$ reduces to the TMDShF, implying that the latter is given by eq. (2.43).

To test the proposed factorization, one may consider another process and check if it is possible to identify the same TMDShF in eq. (3.4). We take into account J/ψ production in hadron collisions, namely $pp \to J/\psi + X$.[4] For this process the small-$\boldsymbol{q}_T$ behavior of the cross section evaluated in the HTM region has been calculated in ref. [18]. The corresponding Sudakov factor can be written as

$$S_A^{pp,\psi}(\boldsymbol{b}_T^2; \mu_H^2) = S_A^g(\boldsymbol{b}_T^2; \mu_H^2) + B_{pp}(\mu_H^2) \log \frac{\mu_H^2}{\mu_b^2}, \tag{3.6}$$

where

$$B_{pp}(\mu_H^2) = -\frac{\alpha_s}{2\pi} C_A \left(1 + 2 \log \frac{\mu_H^2}{M_\psi^2} \right), \tag{3.7}$$

in which the first term of eq. (3.7) is directly related to the δ_{8c} term in ref. [18]. Also in this case we checked that previous equations agree in the kinematic limit corresponding to a bound pair with the open heavy-quark pair production Sudakov factor, which can be found in the literature (for instance ref. [20]). Moreover, even if it is possible to produce quarkonia in a CS state (e.g. η_c), for pp our perturbative tail only applies to CO states.

---

[3]Here we introduced the subscript "ep" to underline that this Δ has been obtained for SIDIS.

[4]It should be mentioned that a J/ψ produced from gg fusion is necessarily in the CO state, because production of a massive CS vector state from two massless gluons is not possible (Landau-Yang theorem). Nevertheless, in case of a CO final state in pp scattering the gluon TMD will involve a different gauge link structure than in ep and TMD factorization may not even hold. As there is much unclear about this, we will ignore this complicating matter in this work.

Despite this, we cannot exclude that a non trivial TMDShF perturbative tail applies to the CS channel too, if one goes to next orders in perturbation theory.

Although the full $\Delta_{pp}^{[n]}$ is different from $\Delta_{ep}^{[n]}$, we can still identify the same $\Delta_{\text{ShF}}^{[n]}$ in eq. (3.4), which is now combined with a different (extra) soft factor S_{pp}, namely

$$\Delta_{pp}^{[n]}(\mu_H^2) = \Delta_{\text{ShF}}^{[n]}(\mu_H^2) \times S_{pp}(\mu_H^2), \tag{3.8}$$

with

$$S_{pp}(\mu_H^2) = 1 + \frac{\alpha_s}{2\pi} C_A \left(3 \log \frac{\mu_H^2}{M_\psi^2} \right) \log \frac{\mu^2}{\mu_b^2} . \tag{3.9}$$

Interestingly, for S_{pp} the coefficient in front of the log is "3", whereas the same coefficient for S_{ep} is "2", which corresponds to the number of TMD quantities (PDFs and shape functions) involved. Hence, even if process dependent, these terms are the same apart from the number of TMDs involved. This may allow to guess the required term for other processes, such as for di-quarkonium production in pp collisions (if that factorizes at all for CO-CO production).

The factor S_{pp} reduces to 1 when $\mu_H = M_\psi$, such that $\Delta_{pp}^{[n]}(M_\psi^2) = \Delta_{\text{ShF}}^{[n]}(M_\psi^2)$. For this scale choice, $\Delta_{\text{ShF}}^{[n]}(M_\psi^2)$ is compatible with the corresponding one presented in ref. [15] for χ_c decay into light-quarks, where the NLO TMDShF up to corrections of $\mathcal{O}(|\boldsymbol{k}_T|^{-1})$ is given by a constant too.

According to our findings, in principle one may obtain the value of $\Delta_{ep}^{[n]}(\widetilde{Q}^2)$ from the experimentally determined $\Delta_{pp}^{[n]}(M_\psi^2) = \Delta_{\text{ShF}}^{[n]}(M_\psi^2)(\neq \Delta_{ep}^{[n]}(M_\psi^2))$, by evolving $\Delta_{\text{ShF}}^{[n]}(M_\psi^2)$ to $\Delta_{\text{ShF}}^{[n]}(\widetilde{Q}^2)$. Hence, we propose a strategy for the extraction of the TMDShF from different processes, relying on their factorizability. For processes where we have a dominant hard scale it is reasonable to expect that by setting μ_H equivalent to it we reduce our uncertainties in the extraction of the TMDShF.[5] Then, this term can be re-used for every process involving J/ψ by evolving $\Delta_{\text{ShF}}^{[n]}$ to the scale μ_H' and combining it with the proper process-dependent extra soft factor $S(\mu_H'^2)$.

For completeness, we mention that the soft factor derived for the open heavy-quark pair production also involves an additional process-dependent factor [35–37] (which is sometimes denoted by Δ, but should not to be confused with ours). This additional factor stems from soft radiation in the $Q\bar{Q}$ production and can in principle even depend on the angle of $\boldsymbol{q}_T$. Hence, it is natural to expect an additional process-dependent soft term in the quarkonium case too. In that sense we expect that our extra soft term S will acquire azimuthal and rapidity dependences if one goes beyond the order and approximation we have considered, as they are present in the Δ quantity of refs. [35, 37].

---

[5]This applies to both pp, where we have only M_ψ, and SIDIS, if $Q \gg M_\psi$ or $Q \ll M_\psi$ (including photoproduction).

4 Conclusions

In this work, we revised the procedure to derive the leading order TMDShF perturbative tail for heavy quarkonium production. We focused on the SIDIS unpolarized cross section, which is parameterized in terms of structure functions. In particular, we considered the cross section evaluated at low q_T and order $\alpha\alpha_s$, which involves the convolution between the gluon TMD-PDF and a general TMDShF, taking the reasonable assumption that factorization holds. This description should match the collinear one at high q_T and order $\alpha\alpha_s^2$ when both are evaluated at intermediate q_T, namely $\Lambda_{\rm QCD} \ll |\boldsymbol{q}_T| \ll \mu_H$. We emphasize that, although the exact choice of μ_H is important from a phenomenological point of view where it is advantageous to extend the intermediate-$\boldsymbol{q}_T$ region, our findings hold for any choice of μ_H.

We show that in the high transverse momentum region, these structure functions present poles when the small-$\boldsymbol{q}_T$ limit is taken. We expect that these poles will be contained in other hard amplitudes concerning inclusive quarkonia production. Therefore, we presented a systematic way to deal with them, showing how they provide non-negligible terms in the expansion at small $\boldsymbol{q}_T$. These terms, neglected in [16, 17], significantly alter our findings of the TMDShF perturbative tail. At variance with previous works, it does not present a logarithmic dependence on the transverse momentum (double-logarithm in $\boldsymbol{b}_T$-space), which makes them different from usual TMD fragmentation functions for light hadron production. However, this non-logarithmic dependence is in agreement with other works [14, 15], and with the Sudakov factors obtained for open heavy-quark pair production in electron-proton and proton-proton collisions.

We remark that our results on the transverse momentum dependence of the TMDShFs hold for every CO quarkonium state with the same quantum numbers as the J/ψ we considered, e.g. $\Upsilon(nS)$ and $\psi(2S)$. The magnitude of TMDShFs can be different though and is determined by the LDMEs. This conclusion holds up to the precision considered, corresponding to the $\alpha\alpha_s^2$ and v^4 orders in the NRQCD double expansion. Moreover, the same considerations apply if we take into account the polarization of the J/ψ, since the kinematics is the same. Namely, we have the same TMDShF perturbative tail for both the longitudinal and transverse J/ψ polarization states. Besides, to check that the same form of the TMDShF applies for observables involving $h_1^{\perp g}$ we would require the computation of the cross section within NRQCD at higher order in α_s, both for polarized and unpolarized J/ψ productions. However, this calculation is still unavailable.

Furthermore, we showed that if we consider the evolution w.r.t. the factorization scale μ, the TMDShFs would have to depend on the hard scale Q too. As it is not reasonable to include this dependence into a quantity that is related to the quarkonium formation solely, we considered a split into two terms: a process-independent quantity that we identify as the universal TMDShF, and an extra process-dependent soft factor. This then allows to make a connection between ep and pp processes, without losing predictability completely. It is also in line with results for open heavy quark production, where extra process dependent soft factors are also required, at least in pp collisions [35, 37].

Despite the process dependence, we showed that it is possible to extract the universal TMDShFs by appropriate choices of scales, which allows to relate different processes. Hence, we expect that with the upcoming Electron-Ion Collider and more data provided by *pp* facilities (e.g. LHC in fixed target mode) extractions of the TMDShFs will become available in the future and new features of heavy quarkonium production will be uncovered.

Acknowledgments

A The additional terms of the effective delta

In this appendix we provide more details on the derivation of eq. (2.25). Via the Laurent expansion in eq. (2.17) we obtained the three terms presented in eq. (2.19). The first integral, $\mathrm{d}\sigma_A$, involves only finite terms in the double limit $\hat{x}', \hat{z} \to 1$. On the contrary, $\mathrm{d}\sigma_B$ and $\mathrm{d}\sigma_C$ include indeterminate terms. These are given by the poles, while other quantities can be Taylor expanded around $\hat{z} = 1$ and $\hat{x}' = 1$; e.g. the quantities $\mathcal{H}_{\mathcal{P}}^{[n];(k)}(\hat{z})$ are decomposed as

$$\mathcal{H}_{\mathcal{P}}^{[n];(k)}(\hat{z}) = \mathcal{H}_{\mathcal{P}}^{[n];(k)}(1) + \sum_m (1 - \hat{z})^m \left.\frac{\mathrm{d}^m \mathcal{H}_{\mathcal{P}}^{[n];(k)}(\hat{z})}{\mathrm{d}\hat{z}^m}\right|_{\hat{z}=1} . \tag{A.1}$$

After the first order, the presence of power of $(1 - \hat{z})^m$ solves the indeterminacy, making the quantity $\frac{(1-\hat{z})^{1+m}}{1-\hat{x}}$ null in the double limit. Hence, one can approximate $\hat{z} = 1$ and $\hat{x}' = 1$ whenever possible, and subsequently perform the analytic integral. To achieve so, we can utilize the solution of $\hat{x}'$ imposed by $\delta(G(\hat{x}', \hat{z}))$, namely

$$\hat{x}'_0 = 1 - \frac{(1 - \hat{z})^2 M_\psi^2 + \hat{z}^2 \boldsymbol{q}_T^2}{(1 - \hat{z})(M_\psi^2 + \hat{z}Q^2) + \hat{z}\boldsymbol{q}_T^2} . \tag{A.2}$$

Hence, via eq. (A.2) we are able to rewrite the denominator of the poles and, subsequently, integrate analytically the remaining function. Explicitly, we have that

$$
\begin{aligned}
\mathrm{d}\sigma_B &\approx \frac{\alpha}{4yQ^2} f^g(x;\mu^2) \sum_n \left[\left(1 + (1-y)^2\right) \mathcal{H}_\perp^{(g)[n];(1)}(1) + 4(1-y)\mathcal{H}_\parallel^{(g)[n];(1)}(1) \right] \langle \mathcal{O}[n] \rangle \\
&\quad \times \int_0^1 \mathrm{d}\hat{x}' \int_0^1 \mathrm{d}\hat{z} \left(\frac{1-\hat{z}}{1-\hat{x}'} \right) \delta(G(\hat{x}',\hat{z})) \delta(1-z) \\
&= \frac{\alpha}{4yQ^2} f^g(x;\mu^2) \sum_n \left[\left(1 + (1-y)^2\right) \mathcal{H}_\perp^{(g)[n];(1)}(1) + 4(1-y)\mathcal{H}_\parallel^{(g)[n];(1)}(1) \right] \langle \mathcal{O}[n] \rangle \\
&\quad \times Q^2 \int_0^1 \mathrm{d}\hat{x}' \int_0^1 \mathrm{d}\hat{z} \left(\frac{1-\hat{z}}{(1-\hat{z})^2 M_\psi^2 + \hat{z}^2 \boldsymbol{q}_T^2} \right) \delta(\hat{x}' - \hat{x}_0') \delta(1-z) \\
&= \frac{\alpha}{4yQ^2} f^g(x;\mu^2) \sum_n \left[\left(1 + (1-y)^2\right) \mathcal{H}_\perp^{(g)[n];(1)}(1) + 4(1-y)\mathcal{H}_\parallel^{(g)[n];(1)}(1) \right] \langle \mathcal{O}[n] \rangle \\
&\quad \times \left(\frac{Q^2}{2M_\psi^2} \log \frac{M_\psi^2}{\boldsymbol{q}_T^2} \right) \delta(1-z) \\
&= \frac{\alpha}{4yQ^2} f^g(x;\mu^2) \sum_n \left[\left(1 + (1-y)^2\right) \mathcal{H}_\perp^{(g)[n];(0)}(1,1) + 4(1-y)\mathcal{H}_\parallel^{(g)[n];(0)}(1,1) \right] \langle \mathcal{O}[n] \rangle \\
&\quad \times \left(-\hat{x}_{\max} \log \frac{M_\psi^2}{\boldsymbol{q}_T^2} \right) \delta(1-z),
\end{aligned}
\tag{A.3}
$$

and

$$
\begin{aligned}
\mathrm{d}\sigma_C &\approx \frac{\alpha}{4yQ^2} f^g(x;\mu^2) \sum_n \left[\left(1 + (1-y)^2\right) \mathcal{H}_\perp^{(g)[n];(2)}(1) + 4(1-y)\mathcal{H}_\parallel^{(g)[n];(2)}(1) \right] \langle \mathcal{O}[n] \rangle \\
&\quad \times \int_0^1 \mathrm{d}\hat{x}' \int_0^1 \mathrm{d}\hat{z} \left(\frac{1-\hat{z}}{1-\hat{x}'} \right)^2 \delta(G(\hat{x}',\hat{z})) \delta(1-z) \\
&= \frac{\alpha}{4yQ^2} f^g(x;\mu^2) \sum_n \left[\left(1 + (1-y)^2\right) \mathcal{H}_\perp^{(g)[n];(2)}(1) + 4(1-y)\mathcal{H}_\parallel^{(g)[n];(2)}(1) \right] \langle \mathcal{O}[n] \rangle \\
&\quad \times Q^2 \int_0^1 \mathrm{d}\hat{x}' \int_0^1 \mathrm{d}\hat{z} \frac{(1-\hat{z})^2 \left[(1-\hat{z})(M_\psi^2 + \hat{z}Q^2) + \hat{z}^2 \boldsymbol{q}_T^2 \right]}{\left[(1-\hat{z})^2 M_\psi^2 + \hat{z}^2 \boldsymbol{q}_T^2\right]^2} \delta(\hat{x}' - \hat{x}_0') \delta(1-z) \\
&\approx \frac{\alpha}{4yQ^2} f^g(x;\mu^2) \sum_n \left[\left(1 + (1-y)^2\right) \mathcal{H}_\perp^{(g)[n];(2)}(1) + 4(1-y)\mathcal{H}_\parallel^{(g)[n];(2)}(1) \right] \langle \mathcal{O}[n] \rangle \\
&\quad \times Q^2 \int_0^1 \mathrm{d}\hat{x}' \int_0^1 \mathrm{d}\hat{z} \frac{(1-\hat{z})^3}{\left[(1-\hat{z})^2 M_\psi^2 + \hat{z}^2 \boldsymbol{q}_T^2\right]^2} \left(M_\psi^2 + Q^2 \right) \delta(\hat{x}' - \hat{x}_0') \delta(1-z) \\
&= \frac{\alpha}{4yQ^2} f^g(x;\mu^2) \sum_n \left[\left(1 + (1-y)^2\right) \mathcal{H}_\perp^{(g)[n];(2)}(1) + 4(1-y)\mathcal{H}_\parallel^{(g)[n];(2)}(1) \right] \langle \mathcal{O}[n] \rangle \\
&\quad \times \left[\frac{M_\psi^2 + Q^2}{M_\psi^2} \frac{Q^2}{2M_\psi^2} \left(\log \frac{M_\psi^2}{\boldsymbol{q}_T^2} - 1 \right) \right] \delta(1-z) \\
&= \frac{\alpha}{4yQ^2} f^g(x;\mu^2) \sum_n \left[\left(1 + (1-y)^2\right) \mathcal{H}_\perp^{(g)[n];(0)}(1,1) + 4(1-y)\mathcal{H}_\parallel^{(g)[n];(0)}(1,1) \right] \langle \mathcal{O}[n] \rangle \\
&\quad \times \left[\frac{\hat{x}_{\max}}{2} \left(\log \frac{M_\psi^2}{\boldsymbol{q}_T^2} - 1 \right) \right] \delta(1-z),
\end{aligned}
\tag{A.4}
$$

where we recall that $x = x_B/\hat{x}_{\max}$. Note how the last lines in eqs. (A.3) and (A.4) are respectively equivalent to what is presented in eqs. (2.22) and (2.23).
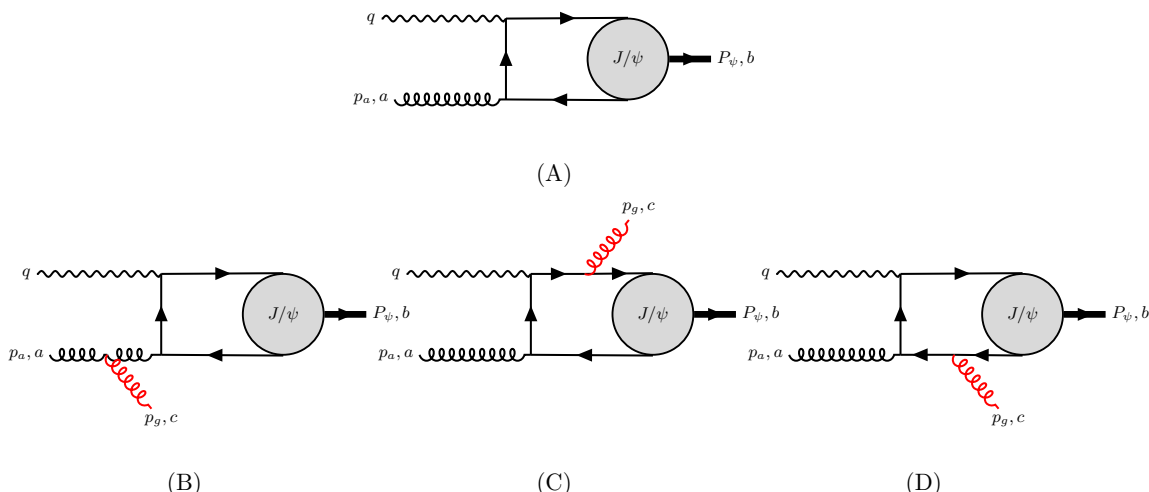
Figure 2. Leading order diagrams for the process $\gamma^* + g \to J/\psi(P_\psi)$, with the inclusion of soft gluon emission (in red) from initial and final states.

B Eikonal method

In this appendix we describe how to evaluate the soft gluon radiation from the leading order partonic subprocess in eq. (2.30) by adopting the eikonal approximation.

The Born amplitude is depicted in figure 2.A and the soft gluon emission is obtained by attaching a (soft) gluon to the initial (hard) gluon, as in figure 2.B, or to the heavy quark-antiquark pair, figures 2.C and 2.D. The eikonal gluon has a four-momentum p_g that is negligible compared to the other (hard) momenta in the process. Hence, its polarization vector $\varepsilon_{\lambda_g}(p_g)$ fulfills the following relation

$$\sum_{\lambda_g} \varepsilon_{\lambda_g}^{*\alpha}(p_g)\varepsilon_{\lambda_g}^{\beta}(p_g) \to -g^{\alpha\beta} \; . \tag{B.1}$$

Moreover, the soft external gluon has color index c and the initial gluon and the outgoing pair have color index a and b, respectively.

The leading order amplitude of figure 2.A is given by

$$\mathcal{M}_0 = \delta_{ab}M_0, \tag{B.2}$$

with

$$M_0 = \int \frac{\mathrm{d}^4k}{(2\pi)^4}\epsilon_{\lambda_a}^{\mu}(p_a)g_{\mu\nu}O_{ij}^{\nu}(P_\psi,k)\Phi_{ji}^{(b)}(P_\psi,k), \tag{B.3}$$

where $\epsilon_{\lambda_a}(p_a)$ is the polarization vector of the incoming gluon, $O(P_\psi,k)$ the perturbative operator related to the hard amplitude and $\Phi^{(b)}(P_\psi,k)$ the wave function of the non-relativistic $c\bar{c}$ pair. Note that we are considering the pair having total momentum P_ψ and relative momentum $2k$, and i and j are the color indices of the quark and antiquark, respectively.

The amplitudes for figures 2.B-2.D, where we have the insertion of an eikonal gluon, are identified by $\mathcal{M}_1^{(I)}$ with $I = B, C, D$. They can be obtained from the Born one in

figure 2.A through proper replacements in a light-cone gauge. Here we list those needed to evaluate $\mathcal{M}_1$:

- Emission from the incoming gluon

$$\epsilon^\mu(p_a) \to -ig_s f_{aa'c} \epsilon^\mu(p_a) \left[(p_a \cdot \epsilon^*_{\lambda_g})/(p_a \cdot p_g) \right]$$
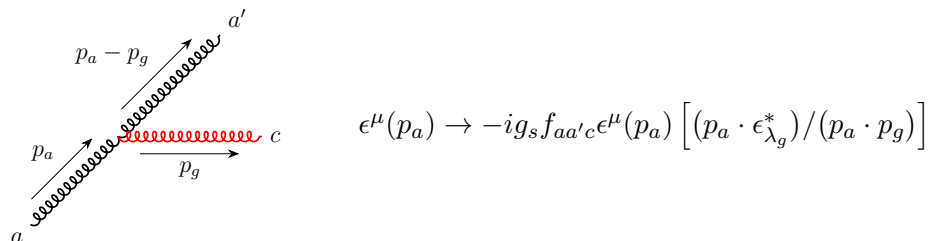
- Emission from the outgoing quarkonia (solely color octet)

$$\Phi_{ji}(P_\psi, k) \to$$
$$-ig_s f_{bb'c} \left[(P_\psi \cdot \epsilon^*_{\lambda_g})/(P_\psi \cdot p_g) \right] \Phi_{ji}(P_\psi, k)$$
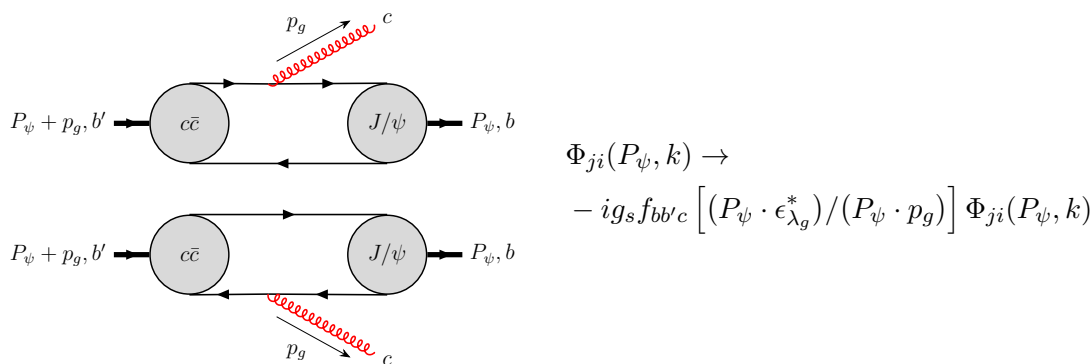
From the first replacement we have that

$$\mathcal{M}_1^{(B)} = \delta_{a'b} M_1^{(B)} = (-ig_s f_{abc}) \varepsilon^{*\alpha}_{\lambda_g}(p_g) \left[\frac{p_{a\alpha}}{p_a \cdot p_g - i\epsilon} \right] M_0, \tag{B.4}$$

which is valid independently from the Fock-state of the $c\bar{c}$ pair, while from the second one we get

$$\mathcal{M}_1^{(C+D)} = \delta_{ab'} M_1^{(C+D)} = (ig_s f_{abc}) \frac{P_{\psi\alpha}}{P_\psi \cdot p_g} \varepsilon^{*\alpha}_{\lambda_g}(p_g) M_0, \tag{B.5}$$

if the bound state is produced in a CO configuration (the relation is still independent of the other quantum numbers). By combining eqs. (B.4) and (B.5) we obtain the full amplitude that includes the soft gluon radiation from both the incoming gluon and the outgoing (CO) $c\bar{c}$ pair, namely

$$\mathcal{M}_1 = (ig_s f_{abc}) \left[\frac{P_{\psi\alpha}}{P_\psi \cdot p_g} - \frac{p_{a\alpha}}{p_a \cdot p_g} \right] \varepsilon^{*\alpha}_{\lambda_g}(p_g) M_0 . \tag{B.6}$$

Averaging over colors and using eq. (B.1), we then find that

$$\overline{|\mathcal{M}_1|}^2 = g_s^2 C_A \left[2S_g(p_a, P_\psi) - S_g(P_\psi, P_\psi) \right] \overline{|M_0|}^2, \tag{B.7}$$

where

$$S_g(v_1, v_2) = \frac{v_1 \cdot v_2}{(v_1 \cdot p_g)(v_2 \cdot p_g)} \ . \tag{B.8}$$

Considering a frame where $\boldsymbol{q}$ and $\boldsymbol{p}_a$ are along the z axis, we can choose two light-cone vectors κ_+^μ and κ_-^μ such that

$$
\begin{aligned}
p_a^\mu &= \frac{x_B}{\hat{x}_{\max}}\kappa_+^\mu, \\
q^\mu &= -x_B\kappa_+^\mu + \frac{Q^2}{2x_B}\kappa_-^\mu, \\
p_g^\mu &= p_g^+\kappa_+^\mu + p_g^-\kappa_-^\mu + p_{g\perp}^\mu = p_g^+\kappa_+^\mu + p_g^-\kappa_-^\mu - P_{\psi\perp}^\mu,
\end{aligned}
\tag{B.9}
$$

where from the momentum conservation we have that $\boldsymbol{P}_{\psi\perp} = -\boldsymbol{p}_{g\perp}$, while by considering the softness of the gluon in the final state $(q + p_a)^2 \approx M_\psi^2$.

We can introduce the variable x_g defined by

$$x_g = \frac{p_g \cdot p_a}{q \cdot p_a} = \frac{2x_B}{Q^2}p_g^-, \tag{B.10}$$

which is also constrained by the momentum conservation

$$\frac{\boldsymbol{p}_{g\perp}^2}{M_\psi^2 + Q^2} \le x_g \le 1 \ . \tag{B.11}$$

Then, the phase space of the emitted (on-shell) soft gluon is given by

$$\frac{\mathrm{d}^4 p_g}{(2\pi)^3}\delta(p_g^2) = \frac{\mathrm{d}^2\boldsymbol{p}_{g\perp}}{2(2\pi)^3}\frac{\mathrm{d}p_g^-}{p_g^-} = \frac{\mathrm{d}^2\boldsymbol{P}_{\psi\perp}}{2(2\pi)^3}\frac{\mathrm{d}x_g}{x_g}, \tag{B.12}$$

and the differential cross section will be proportional to the integration w.r.t. x_g of eq. (B.7), namely[6]

$$\mathrm{d}\sigma_1 \propto \frac{g_s^2}{2(2\pi)^3}C_A \int_{\frac{\boldsymbol{p}_{g\perp}^2}{M_\psi^2+Q^2}}^{1} \frac{\mathrm{d}x_g}{x_g}\Big[2S_g(p_a, P_\psi) - S_g(P_\psi, P_\psi)\Big]\overline{|M_0|}^2 = \frac{g_s^2}{2(2\pi)^3}C_A\Big[2I_a - I_\psi\Big]\overline{|M_0|}^2. \tag{B.13}$$

The argument of the integral reads

$$
\begin{aligned}
S_g(p_a, P_\psi) &= \frac{p_a \cdot P_\psi}{(p_a \cdot p_g)(P_\psi \cdot p_g)} \\
&\approx \frac{p_a \cdot q}{(p_a \cdot p_g)\Big[(p_a \cdot p_g) + (q \cdot p_g)\Big]} = \frac{2}{M_\psi^2 x_g^2 + \boldsymbol{p}_{g\perp}^2},
\end{aligned}
\tag{B.14}
$$

while

$$S_g(P_\psi, P_\psi) = \frac{M_\psi^2}{(P_\psi \cdot p_g)^2} \approx \frac{M_\psi^2}{\Big[(p_a \cdot p_g) + (q \cdot p_g)\Big]^2} = \frac{4M_\psi^2 x_g^2}{(M_\psi^2 x_g^2 + \boldsymbol{p}_{g\perp}^2)^2} \ . \tag{B.15}$$

---

[6]The proportionality is due to the presence of Lorentz-invariant phase spaces, not explicitly shown here.

Hence, we can solve eq. (B.13) analytically finding

$$I_a = \int_{\frac{\boldsymbol{p}_{g\perp}^2}{M_\psi^2 + Q^2}}^1 \frac{\mathrm{d}x_g}{x_g} \frac{2}{M_\psi^2 x_g^2 + \boldsymbol{p}_{g\perp}^2} \approx \frac{1}{\boldsymbol{p}_{g\perp}^2} \left[\log \frac{M_\psi^2 + Q^2}{\boldsymbol{p}_{g\perp}^2} + \log \frac{M_\psi^2 + Q^2}{M_\psi^2} \right] \tag{B.16}$$

and

$$I_\psi = \int_{\frac{\boldsymbol{p}_{g\perp}^2}{M_\psi^2 + Q^2}}^1 \frac{\mathrm{d}x_g}{x_g} \frac{4M_\psi^2 x_g^2}{\left(M_\psi^2 x_g^2 + \boldsymbol{p}_{g\perp}^2\right)^2} \approx \frac{2}{\boldsymbol{p}_{g\perp}^2}, \tag{B.17}$$

so that

$$\mathrm{d}\sigma_1 \propto \frac{\alpha_s}{2\pi^2 \boldsymbol{p}_{g\perp}^2} C_A \left[\log \frac{M_\psi^2 + Q^2}{\boldsymbol{p}_{g\perp}^2} + \log \frac{M_\psi^2 + Q^2}{M_\psi^2} - 1 \right] \overline{|M_0|}^2 \tag{B.18}$$

is in agreement with the first term of eq. (2.27).

Open Access. This article is distributed under the terms of the Creative Commons Attribution License (CC-BY 4.0), which permits any use, distribution and reproduction in any medium, provided the original author(s) and source are credited.

References

[1] R.M. Godbole, A. Misra, A. Mukherjee and V.S. Rawoot, *Sivers Effect and Transverse Single Spin Asymmetry in $e + p^\uparrow \to e + J/\psi + X$*, *Phys. Rev. D* **85** (2012) 094013 [arXiv:1201.1066] [INSPIRE].

[2] D. Boer and C. Pisano, *Polarized gluon studies with charmonium and bottomonium at LHCb and AFTER*, *Phys. Rev. D* **86** (2012) 094007 [arXiv:1208.3642] [INSPIRE].

[3] R.M. Godbole, A. Misra, A. Mukherjee and V.S. Rawoot, *Transverse Single Spin Asymmetry in $e + p^\uparrow \to e + J/\psi + X$ and Transverse Momentum Dependent Evolution of the Sivers Function*, *Phys. Rev. D* **88** (2013) 014029 [arXiv:1304.2584] [INSPIRE].

[4] W.J. den Dunnen, J.P. Lansberg, C. Pisano and M. Schlegel, *Accessing the Transverse Dynamics and Polarization of Gluons inside the Proton at the LHC*, *Phys. Rev. Lett.* **112** (2014) 212001 [arXiv:1401.7611] [INSPIRE].

[5] A. Mukherjee and S. Rajesh, *Probing Transverse Momentum Dependent Parton Distributions in Charmonium and Bottomonium Production*, *Phys. Rev. D* **93** (2016) 054018 [arXiv:1511.04319] [INSPIRE].

[6] A. Mukherjee and S. Rajesh, *Linearly polarized gluons in charmonium and bottomonium production in color octet model*, *Phys. Rev. D* **95** (2017) 034039 [arXiv:1611.05974] [INSPIRE].

[7] A. Mukherjee and S. Rajesh, *J/ψ production in polarized and unpolarized ep collision and Sivers and $\cos 2\phi$ asymmetries*, *Eur. Phys. J. C* **77** (2017) 854 [arXiv:1609.05596] [INSPIRE].

[8] S. Rajesh, R. Kishore and A. Mukherjee, *Sivers effect in Inelastic J/ψ Photoproduction in $ep^\uparrow$ Collision in Color Octet Model*, *Phys. Rev. D* **98** (2018) 014007 [arXiv:1802.10359] [INSPIRE].

[9] F. Scarpa et al., *Studies of gluon TMDs and their evolution using quarkonium-pair production at the LHC*, *Eur. Phys. J. C* **80** (2020) 87 [arXiv:1909.05769] [INSPIRE].

[10] U. D'Alesio, F. Murgia, C. Pisano and P. Taels, *Azimuthal asymmetries in semi-inclusive* J/ψ + jet *production at an EIC*, *Phys. Rev. D* **100** (2019) 094016 [arXiv:1908.00446] [INSPIRE].

[11] R. Kishore, A. Mukherjee and M. Siddiqah, *Cos(2φ_h) asymmetry in J/ψ production in unpolarized ep collision*, *Phys. Rev. D* **104** (2021) 094015 [arXiv:2103.09070] [INSPIRE].

[12] A. Bacchetta, D. Boer, C. Pisano and P. Taels, *Gluon TMDs and NRQCD matrix elements in J/ψ production at an EIC*, *Eur. Phys. J. C* **80** (2020) 72 [arXiv:1809.02056] [INSPIRE].

[13] G.T. Bodwin, E. Braaten and G.P. Lepage, *Rigorous QCD analysis of inclusive annihilation and production of heavy quarkonium*, *Phys. Rev. D* **51** (1995) 1125 [*Erratum ibid.* **55** (1997) 5853] [hep-ph/9407339] [INSPIRE].

[14] M.G. Echevarria, *Proper TMD factorization for quarkonia production:* $pp \to \eta_{c,b}$ *as a study case*, *JHEP* **10** (2019) 144 [arXiv:1907.06494] [INSPIRE].

[15] S. Fleming, Y. Makris and T. Mehen, *An effective field theory approach to quarkonium at small transverse momentum*, *JHEP* **04** (2020) 122 [arXiv:1910.03586] [INSPIRE].

[16] D. Boer et al., *J/ψ meson production in SIDIS: matching high and low transverse momentum*, *JHEP* **09** (2020) 040 [arXiv:2004.06740] [INSPIRE].

[17] U. D'Alesio et al., *J/ψ polarization in semi-inclusive DIS at low and high transverse momentum*, *JHEP* **03** (2022) 037 [arXiv:2110.07529] [INSPIRE].

[18] P. Sun, C.-P. Yuan and F. Yuan, *Heavy Quarkonium Production at Low Pt in NRQCD with Soft Gluon Resummation*, *Phys. Rev. D* **88** (2013) 054008 [arXiv:1210.3432] [INSPIRE].

[19] R. Zhu, P. Sun and F. Yuan, *Low Transverse Momentum Heavy Quark Pair Production to Probe Gluon Tomography*, *Phys. Lett. B* **727** (2013) 474 [arXiv:1309.0780] [INSPIRE].

[20] H.X. Zhu et al., *Transverse-momentum resummation for top-quark pairs at hadron colliders*, *Phys. Rev. Lett.* **110** (2013) 082001 [arXiv:1208.5774] [INSPIRE].

[21] M.G. Echevarria, *Probing TMDs with quarkonium production*, Talk19219 (2022).

[22] J. Bor and D. Boer, *TMD evolution study of the* $\cos 2\phi$ *azimuthal asymmetry in unpolarized J/ψ production at EIC*, *Phys. Rev. D* **106** (2022) 014030 [arXiv:2204.01527] [INSPIRE].

[23] R. Meng, F.I. Olness and D.E. Soper, *Semiinclusive deeply inelastic scattering at small* q_T, *Phys. Rev. D* **54** (1996) 1919 [hep-ph/9511311] [INSPIRE].

[24] B.A. Kniehl and L. Zwirner, *J/ψ inclusive production in ep deep inelastic scattering at DESY HERA*, *Nucl. Phys. B* **621** (2002) 337 [hep-ph/0112199] [INSPIRE].

[25] Z. Sun and H.-F. Zhang, *QCD leading order study of the J/ψ leptoproduction at HERA within the nonrelativistic QCD framework*, *Eur. Phys. J. C* **77** (2017) 744 [arXiv:1702.02097] [INSPIRE].

[26] J. Collins, *Foundations of perturbative QCD*, Cambridge University Press (2013).

[27] P. Sun, B.-W. Xiao and F. Yuan, *Gluon Distribution Functions and Higgs Boson Production at Moderate Transverse Momentum*, *Phys. Rev. D* **84** (2011) 094005 [arXiv:1109.1354] [INSPIRE].

[28] S. Catani and M. Grazzini, *QCD transverse-momentum resummation in gluon fusion processes*, *Nucl. Phys. B* **845** (2011) 297 [arXiv:1011.3918] [INSPIRE].

[29] Z.-B. Kang, Y.-Q. Ma, J.-W. Qiu and G. Sterman, *Heavy Quarkonium Production at Collider Energies: Partonic Cross Section and Polarization*, *Phys. Rev. D* **91** (2015) 014030 [arXiv:1411.2456] [INSPIRE].

[30] Y.-Q. Ma, J.-W. Qiu, G. Sterman and H. Zhang, *Factorized power expansion for high-p_T heavy quarkonium production*, *Phys. Rev. Lett.* **113** (2014) 142002 [arXiv:1407.0383] [INSPIRE].

[31] Z.-B. Kang, Y.-Q. Ma, J.-W. Qiu and G. Sterman, *Heavy Quarkonium Production at Collider Energies: Factorization and Evolution*, *Phys. Rev. D* **90** (2014) 034006 [arXiv:1401.0923] [INSPIRE].

[32] K. Lee, J.-W. Qiu, G. Sterman and K. Watanabe, *QCD factorization for hadronic quarkonium production at high p_T*, *SciPost Phys. Proc.* **8** (2022) 143 [arXiv:2108.00305] [INSPIRE].

[33] R.F. del Castillo, M.G. Echevarria, Y. Makris and I. Scimemi, *Transverse momentum dependent distributions in dijet and heavy hadron pair production at EIC*, *JHEP* **03** (2022) 047 [arXiv:2111.03703] [INSPIRE].

[34] M.G. Echevarria, T. Kasemets, P.J. Mulders and C. Pisano, *QCD evolution of (un)polarized gluon TMDPDFs and the Higgs q_T-distribution*, *JHEP* **07** (2015) 158 [*Erratum ibid.* **05** (2017) 073] [arXiv:1502.05354] [INSPIRE].

[35] S. Catani, M. Grazzini and A. Torre, *Transverse-momentum resummation for heavy-quark hadroproduction*, *Nucl. Phys. B* **890** (2014) 518 [arXiv:1408.4564] [INSPIRE].

[36] S. Catani, I. Fabre, M. Grazzini and S. Kallweit, *$t\bar{t}H$ production at NNLO: the flavour off-diagonal channels*, *Eur. Phys. J. C* **81** (2021) 491 [arXiv:2102.03256] [INSPIRE].

[37] W.-L. Ju and M. Schönherr, *Projected transverse momentum resummation in top-antitop pair production at LHC*, *JHEP* **02** (2023) 075 [arXiv:2210.09272] [INSPIRE].